Kinetics And Mechanism Of Thermal Decomposition Of Binary Mixture Of Ferrous Oxalate And Copper Oxalate In The (1:2) Mole Ratio

*S. K. Zaware And S. S. Jadhav**
Department of Chemistry, New Arts, Commerce and Science College, Ahmednagar-414001 (MS) INDIA

Abstract

The non-isothermal decomposition study of individual $FeC_2O_4.2H_2O$ shows two steps decomposition with Fe_2O_3 as final product when heated to 300 °C with two dimensional diffusion and Ginling Braunshtein equation. The CuC_2O_4 shows two steps decomposition with CuO as end product when heated to 320 °C by Avrami equation. The non-isothermal study of the binary mechanical mixture of $FeC_2O_4.2H_2O$ and CuC_2O_4 in mole ratio (1:2) by TGA when heated up to 260 °C shows mixture of Fe_2O_3 and CuO. The α Vs time plots of isothermal study of mixture shows Ginling Braunshtein equation and Mampel unimolecular law. The applicability of Mampel unimolecular law to the kinetic data is up to $0.28 < \alpha < 1.00$. The end products were characterized using X-ray diffraction and SEM technique. The kinetic parameters like energy of activation (Ea), pre-exponential factor (A) and Correlation factor (r) were obtained from isothermal TGA and EGA.

***Keywords**: FeC_2O_4 . CuC_2O_4 . TGA . EGA . Kinetics.*

1. Introduction

The thermal stability of solid materials is of great importance and interest [1]. Decomposition of metal oxalates provides a means of comparing the influence of the metal ion on decomposition [2]. Thermal decomposition study of metal oxalates is useful for preparation of mixed metal oxides possessing pores, lattice imperfections and therefore they acts as reactive solids [3]. One of the most convenient measures of the reactivity of a solid is its thermal behavior and pre-treatment like studied at selected isothermal temperatures, which can modify the properties of the material in an important way by creating imperfections and affect on kinetics of decomposition [4]. The mixed metal oxides may result in the modification of their thermal behavior, geometry and electronic properties which lead to changes in their catalytic functions [5]. It is found that many workers studied thermal decomposition of mixed metal oxalates preparing them by different techniques [6]. The objective of this work is to investigate the mechanism by which metal oxalate shows thermal decomposition. So far, nobody appears to have reported on the thermal behavior of mechanical mixtures of $FeC_2O_4.2H_2O$ and CuC_2O_4 in (1:2) mole ratio. Generally, the kinetics of solid state thermal decomposition can be followed either by isothermal and non-isothermal methods [7]. In last few years some workers have studied the binary mixtures of oxalates by thermal decomposition to find out the kinetics and mechanism [8]**,** but we have chosen quite new method to study the binary mixture by mechanically mixing two oxalates by definite proportion as 1:1, 1:2 ,2:1, 1:3 etc. The effect of mixing on the kinetic parameters of individual oxalates is to be studied. The decomposition in oxalates may be with the heterolytic dissociation of C-C bond forming CO_2 and CO_2^{2-} , if it involves the cleavage of the C-C bond then the products are CO and CO_2. In many cases the C-C bond cleavage is the rate determining step. If cleavage is heterolytic then it produces CO_2 and CO_2^{2-} and if hemolytic then it produces two CO^{2-} anions [9-12]. Non-isothermal thermo-gravimetric analysis (TGA) has been widely used as a tool to investigate the thermal stability of complexes [13]. Thermo-gram obtained, provide the information about the sample composition, thermal stability as well as the kinetic data relating the chemical changes occur on heating [14]. The kinetic parameters of non-isothermal method of TGA and EGA are close to those obtained for isothermal decomposition in the air atmosphere. EGA is known as one of thermal analysis method for measuring the amount of generated gases from a sample as a function of temperature [15]. The kinetic analysis data was performed by using computer for calculation of energy of activation and mechanism. The product remains after thermal decomposition of

oxalate mixture was characterized by using X-ray diffraction techniques [16].

2. Experimental

2.1 Material

Pure Ferrous (II) oxalate and Copper (II) oxalate were used of BDH A. R. quality.

2.2 Apparatus

The EGA technique in which furnace is made up of indigenous material with quartz tube closed from one side is used and chromel-alumel is used as thermocouple. Pyrometer (Tempo Industrial corp., BPL-INDIA) with range 0^0C to 1200^0C (± 0.1°C) and the temperature regulator (Argo transformers Co.Ltd., India) of 15 amp capacity is used. In the non-isothermal studies the temperature was raised upto1000 °C at heating rates of 5 °C/min. The TGA K-14 super (K.Roy and Co., India) of 100g capacity with an accuracy of ± 0.1mg is used and non-isothermal and isothermal TGA were carried out with the same thermobalance. The DTA technique Detector DTG-60H is used where atmosphere is air and flow rate is 50ml/min.

X-ray powder diffraction analysis of the solid decomposition products was carried out using a bruker axs D8 advance X-ray diffractometer. For the identification purpose, the relative intensities (I/I_0) and the d-spacing (Å) were compared with standard diffraction patterns of the ASTM powder diffraction files [17].

The changes in morphology and texture taking place during the thermal decomposition of the mixture were investigated using a 6360 (LA) scanning electron microscope.

2.3 Data analysis:

The activation parameters were then calculated by using the Coats-Redfern equation written in the form:

$$\log_{10}\{1-(1-\alpha)^{1-n}/T^2(1-n\}=\log_{10}AR/aE[1-2RT/E]-E/2.303RT \quad \textbf{(1)}$$

Where α = the fraction of the sample decomposed at time t

n = the order of reaction

T = temperature (^{0}K)

A= pre-exponential factor

R = the gas constant

E = the activation energy

a = conversion factor to transfer from a time scale to a temperature scale,

i.e. a = dT / dt

In Coats-Redfern equation $\log_{10}AR/aE$ [1-2RT / E] remains constant over temperature range of the decomposition, then plot

$\log_{10}\{1-(1-\alpha)^{1-n}/T^2(1-n\}$ against 1 / T

It results straight line and slope give the value of –E / 2.303 R [18].

For isothermal conditions, the rate expression can be written as

$$G(\alpha) = kt \text{ (integral form)} \quad \textbf{(2)}$$

α = the fraction of the sample decomposed at time t

For a given isothermal run at T_i, the constant k (T_i) can be calculated from the TGA and EGA Curve using the integral method. TGA and EGA experiments for isothermal analysis are performed at five isothermal temperatures. There is a certain k (T_i) and certain f (α) or G (α) for each T_i. If f (α) or G (α) are all the same for each T_i, then

$$\ln [G(\alpha) / 1.921503T] = \ln (AE / BR) + 3.7720501 - 1.921503 \ln E - E / RT \quad (3)$$

Where

E = slope x R

And

$$A = \exp(\text{intercept} - 3.772051 + 1.9215031 \ln E) \times BR / E \quad (4)$$

Where E = activation energy, B = heating rate, A = frequency factor, and α = the fraction of the sample decomposed at time‘t’ [19].

A computer program has been written for the calculation of kinetic data by using Coats-Redfern equation, in which data can be cycled for any value of n (order of reaction) until the best fit is obtained (by least mean squares) . The kinetic data is also analyzed by two dimensional diffusion equation and by three dimensional phase boundary reaction (Table 1). Plots for typical experiments are shown for non-isothermal TGA, EGA and DTA of $FeC_2O_4.2H_2O$, CuC_2O_4 and binary mechanical mixture of $FeC_2O_4.2H_2O$ and CuC_2O_4 in mole ratio (1:2) in **Figure1**, **Figure2** and **Figure3.**

3. Result and discussion:-

3.1. DTA-TG, EGA

The TGA, EGA and DTA of $FeC_2O_4.2H_2O$ are shown in **Figure 1**. The TGA shows two distinct steps. The first step is observed in the temperature range 180 °C to 200 °C and is accompanied with 20.03% mass loss [20]. This is attributed to the water loss, equivalent to two water molecules (calculated mass loss 20.01%). The second step is occur in the temperature range 240 °C

to 300 °C showing weight loss 45.19% against the calculated mass loss 45.18% [21]. This mass loss corresponds to the complete conversion of FeC_2O_4 to Fe_2O_3. The anhydrous mixture is used for EGA study. EGA shows the theoretical volume for decomposition at N.T.P condition is to be 47.55 ml against the observed volume at N.T.P is 48.00 ml which results in decomposition of FeC_2O_4 to Fe_2O_3 at 380 °C [22]. The DTA shows sharp 'Endo' pick at 200 °C for loss of water of crystallization and second sharp 'Exo' peak at 250 °C for decomposition of FeC_2O_4.

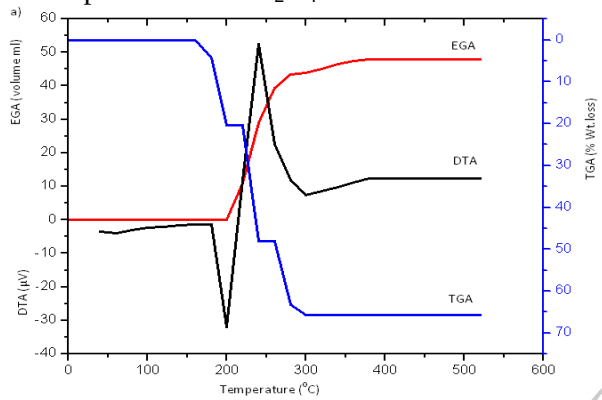

Figure1. DTA-TGA-EGA curves of $FeC_2O_4.2H_2O$ in air at heating rate of 4 °C min^{-1}.

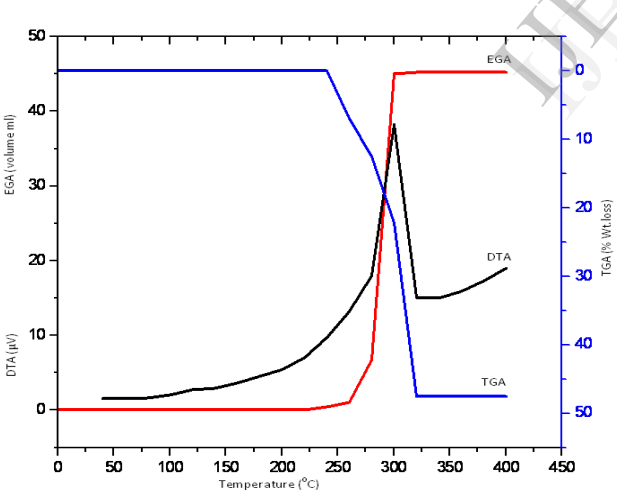

Figure2. DTA-TGA-EGA curves of CuC_2O_4 in air at heating rate of 4 °C min^{-1}.

The TGA, EGA and DTA of CuC_2O_4 are shown in **Figure 2**. The TGA shows single step decomposition in the temperature range 260 °C to 320 °C showing weight loss 47.50% against the calculated mass loss 47.51% [23-24]. This mass loss corresponds to the complete conversion of CuC_2O_4 to CuO. EGA shows the theoretical volume for decomposition at N.T.P condition is to be 45.02 ml against the observed volume at N.T.P is 45.25 ml which results in decomposition of CuC_2O_4 to CuO at 320 °C. The DTA shows sharp 'Exo' peak at 300 °C for decomposition of CuC_2O_4. The kinetic parameters evaluated by TGA using non-mechanistic equations are given in **Table 2**.

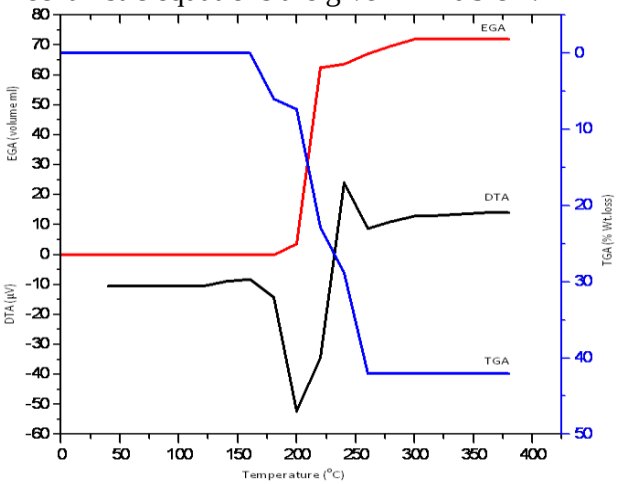

Figure3. DTA-TGA-EGA curves of $FeC_2O_4.2H_2O$ and CuC_2O_4 in mole ratio (1:2) in air at heating rate of 4 °C min^{-1}

In the mixture of $FeC_2O_4.2H_2O$ and CuC_2O_4 in mole ratio (1:2) (**Figure 3**) shows two distinct mass loss steps. The dehydration is observed in the temperature range 120 °C to 200 °C, this is attributed to the two water molecules loss and is accompanied by 7.41% mass loss (calculated mass loss 7.45%) [25]. Anhydrous mixture is thermally unstable and shows decomposition in the temperature range 220 °C to 260 °C to Fe_2O_3 and 2CuO with observed mass loss is 42.02% and calculated mass loss is 42.06 % [26]. The binary mixture shows the initiation temperature 220 °C, which is very less than that of pure $FeC_2O_4.2H_2O$ and CuC_2O_4 which have initiation temp 240 °C and 260 °C, While ends of temperatures are 300 °C and 320 °C respectively. Thus there is appreciable lowering in initiation and end up of temperature of binary mixture is observed. This is due to the fact that the electro-negativity of ferrous oxalate (1.8) is lower than that of Copper oxalate (1.9); addition of ferrous ions to CuC_2O_4 will increase positive charge of the copper ion due to that Cu-O covalent bond becomes weaker in mixed oxalate than pure oxalate.

This makes lower the decomposition temperature and activation energy [27]. The X-ray study of product of mixture at different temperatures (**Figure 4**) supports the formation of $Fe_2Cu_2O_5$. This occurs at lower temperature than the decomposition of pure FeC_2O_4 and CuC_2O_4 due to presence of CuO, which acts as catalyst. EGA study shows the volume for decomposition at N.T.P condition is 72.16 ml and observed volume at N.T.P is 72.00 ml [28], which results in decomposition of FeC_2O_4 and CuC_2O_4 (1:2) mole ratio mixture to Fe_2O_3 and CuO at 300 °C The DTA shows sharp 'Endo' pick at 200 °C for loss of water of crystallization and second sharp 'Exo' peak at 260 °C for decomposition of $FeC_2O_4.2H_2O$ and CuC_2O_4 in mole ratio (1:2) to Fe_2O_3 and CuO [29].

Table1: Kinetic equations examined in this work.

Reaction model	G (α)	Symbol
One dimensional diffusion	α^2	D_1
Two dimensional diffusion	(1-α) ln (1- α) + α	D_2
Jander equation, Three dimensional diffusion	$[1- (1-\alpha)^{1/3}]^2$	D_3
Ginling Braunshtein equation, Three dimensional diffusion	$[1- 2\alpha / 3] -(1-\alpha)]^{2/3}$	D_4
Two dimentional phase boundary reaction.	$[1 – (1-\alpha)^{1/2}]$	R_2
Three dimensional phase boundary reaction.	$[1 – (1-\alpha)^{1/3}]$	R_3
First order kinetics, Mampel unimolecular law, Random nucleation.	[- ln (1-α)]	F_1
Random nucleation: Avrami equation.	$[– \ln (1-\alpha)]^{1/2}$	A_2
Random nucleation: Erofeev equation	$[– \ln (1-\alpha)]^{1/3}$	A_3
Exponential law	ln α	E_1

3.2 X-ray diffraction

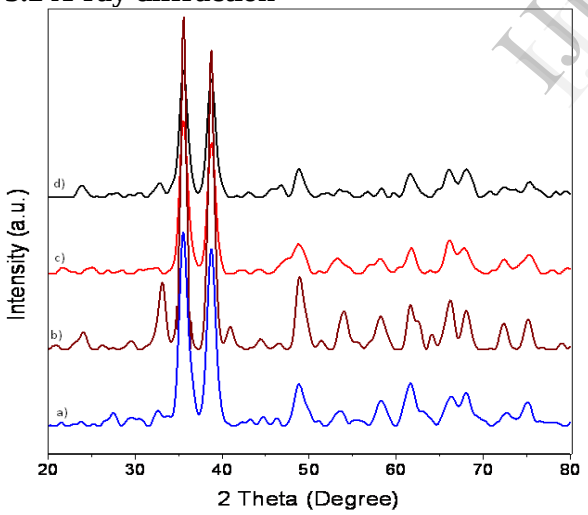

Fig4. X-ray powder diffractograms of solid $FeC_2O_4.2H_2O$ and CuC_2O_4 (1:2) mole ratio mixture obtained at a) 220 °C, b) 230 °C , c) 240 °C , d) 260 °C.

The sample of $FeC_2O_4.2H_2O$ and CuC_2O_4 in mole ratio (1:2) is heated in an open air at 260 °C with a linear heating rate of 4 °C/ min and their XRD pattern is recorded in 2θ range of 20-80^0. The XRD pattern of the sample (**Figure 4**) at 220 °C is matched with monoclinic CuO (JCPDS NO -050661) [30] and cubic $Fe_2Cu_2O_5$ (JCPDS NO-250283) shows that the formation of CuO takes place and not Fe_2O_3, indicates CuO acts as catalyst formed at 220 °C supported by the activation energy (Ea) of pure ferrous (II) oxalate using non-isothermal TGA is 176.33 KJ/mole and pure copper (II) oxalate using non-isothermal TGA is 140.46 KJ/mole, The comparison of average of activation energy (Ea) of both oxide and that of binary mixture in mole ratio (1:2) using non-isothermal TGA is 144.5 KJ/mole shows decrease in activation energy (Ea). The CuO is then further decomposes the mixture at lower temperature. The XRD pattern of the sample at temperature 230 °C, 240 °C, 260 °C shows the formation of hexagonal Fe_2O_3 (JCPDS NO-730603) [31] with cubic $Fe_2Cu_2O_5$ (JCPDS NO-250283) and this phase is found to be not reported.

3.3 Scanning electron microscope

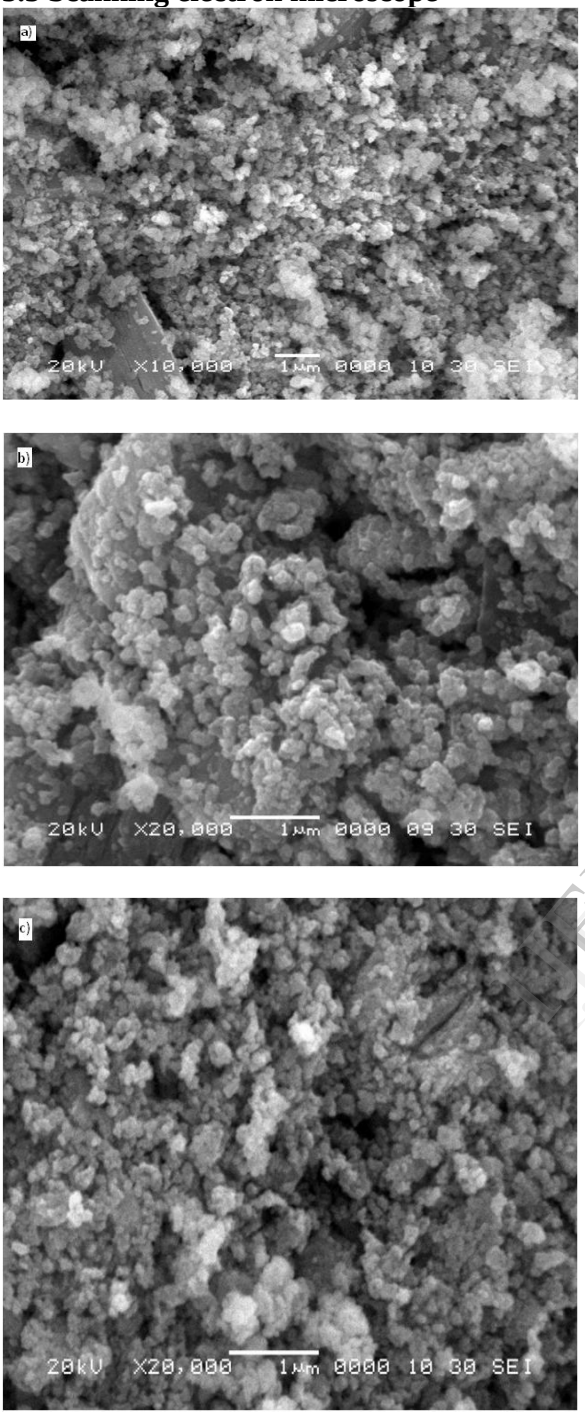

Fig5. Scanning electron micrograph showing the changes in texture and morphology that accompany the thermal decomposition of $FeC_2O_4.2H_2O$ and CuC_2O_4 (1:2) mole ratio mixture in air. Mixture calcined at: a) 220 °C, b) 240 °C, and d) 260 °C.

The SEM micrographs showing the changes in texture and morphology that accompany the thermal decomposition of $FeC_2O_4.2H_2O$ and CuC_2O_4 (1:2) mole ratio mixture in air is shown in (**Figure 5**). The result shows that the particle shape and size change throughout the decomposition process. Micrograph of the mixture is calcined at 220 °C (**Figure 5a)** shows two types of crystals. The first type is due to the decomposition of copper oxalate and breaking into fine granules. The second type shows relatively large crystals of different size and shape, assigned to ferrous oxalate. Micrograph of the mixture is calcined at 240 °C and 260 °C (**Figure 5b and 5c)** shows grain growth, re-texturing and aggregates of cubic large crystals of different sizes. The results of SEM experiments are thus consistent with the result of XRD analysis [32].

3.4. Reaction of mixture

Reaction of $FeC_2O_4.2H_2O$ and CuC_2O_4 in mole ratio (1:2) is shown below.

Step I

$$FeC_2O_4.2H_2O{:}2CuC_2O_4 \xrightarrow{180\ ^\circ C\text{-}200\ ^\circ C} FeC_2O_4{:}2CuC_2O_4{+}2H_2O$$

(Observed Wt. loss = 7.41%), (Calculated Wt. loss = 7.45%)

Step II

$$FeC_2O_4{:} \xrightarrow{220\ ^\circ C\text{-}260\ ^\circ C} 2CuC_2O_4$$

$Fe_2O_3{:}\ 2CuO + 4CO\uparrow + 2CO_2\uparrow$

(Observed Wt. loss = 42.02%), (Calculated Wt. loss = 42.06%)

Five different temperatures 260, 250, 240, 230, 220 °C are selected for conducting isothermal kinetic study of mixture by TGA and 300, 275, 250, 225, and 200 °C for EGA techniques. TGA and EGA (**Figure 5** and **Figure 6**) shows the variation of degree of decomposition (α) of the mixture $FeC_2O_4.2H_2O$ and CuC_2O_4 in (1:2) mole ratio to Fe_2O_3 and 2CuO with time at different isothermal conditions [33]. The data obtained from isothermal method using TGA and EGA techniques are plotted as degree of decomposition (α) as a function of time ($t/t_{0.5}$) (**Figure 7** and **Figure 8**). These sigmoid shaped curves are characteristics of a mechanism by which the decomposition occurs at the interface between the product and un-decomposed reactant.

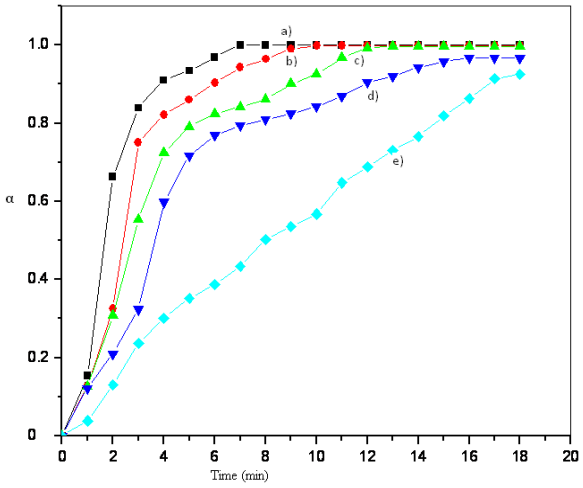

Fig 6. Isothermal decomposition curves (TGA) for $FeC_2O_4.2H_2O$ and CuC_2O_4 (1:2) mole ratio mixture at a)260 °C, b) 250 °C, c) 240 °C, d) 230 °C and e) 220 °C.

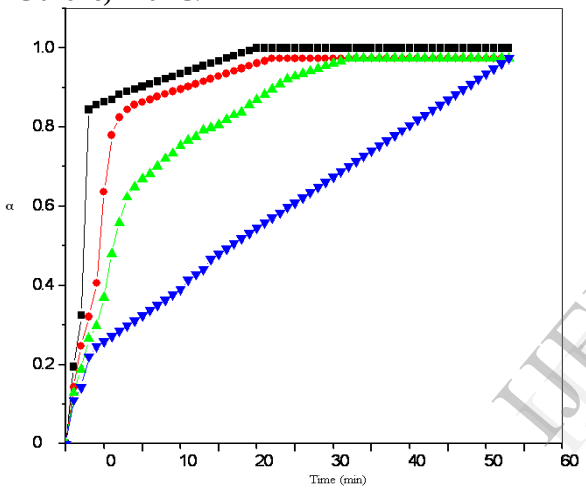

Fig7. Isothermal decomposition curves (EGA) for $FeC_2O_4.2H_2O$ and CuC_2O_4 (1:2) mole ratio mixture at a) 300^0C, (b) 275 ^{0} C c) 250 ^{0}C, and d) 225 ^{0}C.

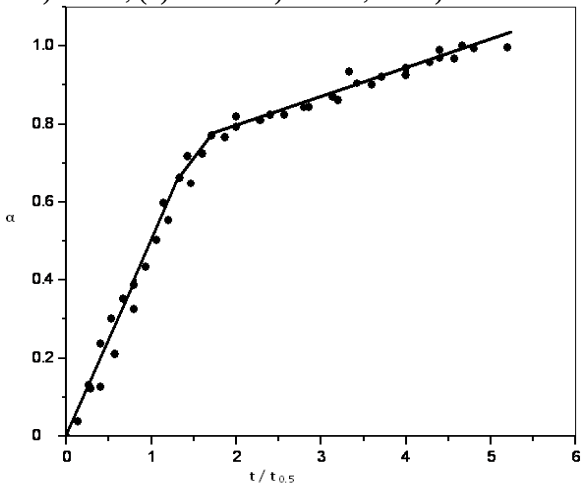

Fig8. α Vs. t / $t_{0.5}$ plots of TGA for isothermal decomposition of $FeC_2O_4.2H_2O$ and CuC_2O_4 (1:2) mole ratio.

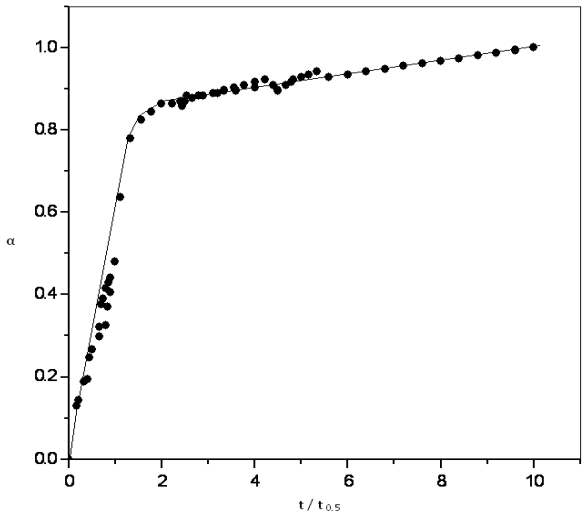

Fig9. α Vs. t / $t_{0.5}$ plots of EGA for isothermal decomposition of $FeC_2O_4.2H_2O$ and CuC_2O_4 (1:2) mole ratio

The kinetic parameters evaluated by TGA using non-mechanistic equations are given in Table 3. The Ea of decomposition process using non-isothermal TGA and EGA method is found 144.35 KJ/mole and 124.81 KJ/mole by plotting ln k Vs. $T^{-1}.10^3/K^{-1}$ respectively (Figure 9 and Figure 10) [34-37]. The order (n) of decomposition reaction of binary mixture using TGA and EGA is 0.45 and 1.30 respectively **[38].**

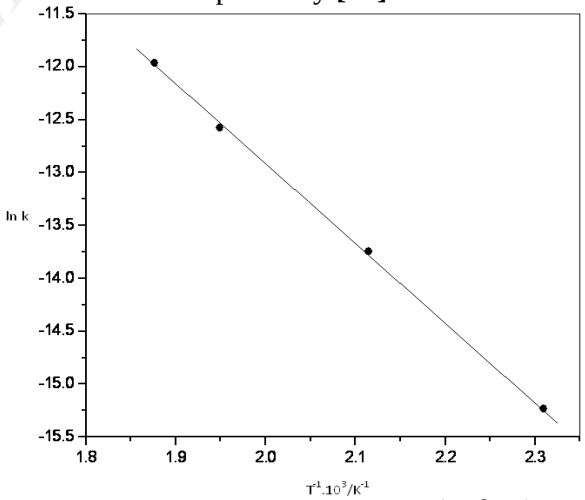

Fig10. Arrhenius plot: of ln k Vs. $T^{-1}.10^3/K^{-1}$ of dynamic TGA of $FeC_2O_4.2H_2O$ and CuC_2O_4 (1:2) mole ratio.

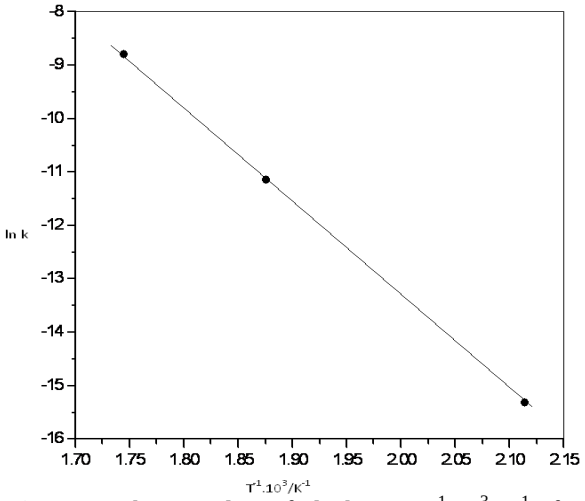

Fig11. Arrhenius plot: of ln k Vs. $T^{-1}.10^3/K^{-1}$ of dynamic EGA of $FeC_2O_4.2H_2O$ and CuC_2O_4 (1:2) mole ratio.

The Ea of isothermal TGA method using three dimensional diffusion (Ginling Braunshtein equation) is 141.51 KJ/mole and first order kinetics (Mampel unimolecular law) or random nucleation is 177.29 KJ/mole by plotting log [1- 2α / 3] – (1-α)] $^{2/3}$ Vs $T^{-1}.10^3/K^{-1}$ and log [- ln (1-α)] Vs. $T^{-1}.10^3/K^{-1}$ (Figure 11 and Figure 12) respectively. The EGA method using three dimensional diffusion (Ginling Braunshtein equation) is 95.17 KJ/mole and first order kinetics (Mampel unimolecular law) i.e random nucleation is 129.41 KJ/mole by plotting log [1- 2α / 3] –(1-α)] $^{2/3}$ Vs $T^{-1}.10^3/K^{-1}$ and log [- ln (1-α)] Vs. $T^{-1}.10^3/K^{-1}$ (Figure 13 and Figure 14) respectively [39]. In EGA technique the decomposition temperature and Ea (activation energy) is high due to closed system. The correlation coefficient (r) for TGA and EGA is in the range 0.9993 - 0.9999, indicating nearly perfect fits [40].

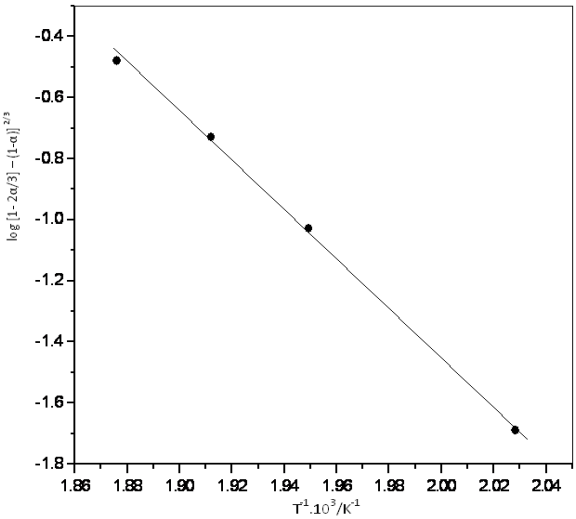

Fig12. Arrhenius plot for TGA of log [1- 2α/3] – (1-α)] $^{2/3}$ Vs $T^{-1}.10^3/K^{-1}$ for decomposition of $FeC_2O_4.2H_2O$ and CuC_2O_4 (1:2) mole ratio.

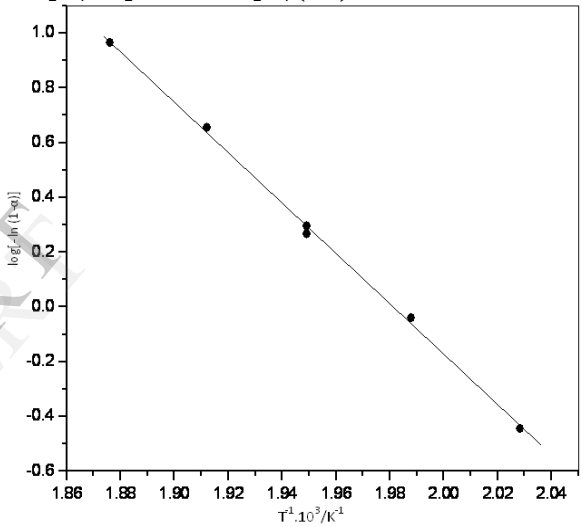

Fig13. Arrhenius plot for TGA of log [- ln (1-α)] Vs $T^{-1}.10^3/K^{-1}$ for decomposition of $FeC_2O_4.2H_2O$ and CuC_2O_4 (1:2) mole ratio

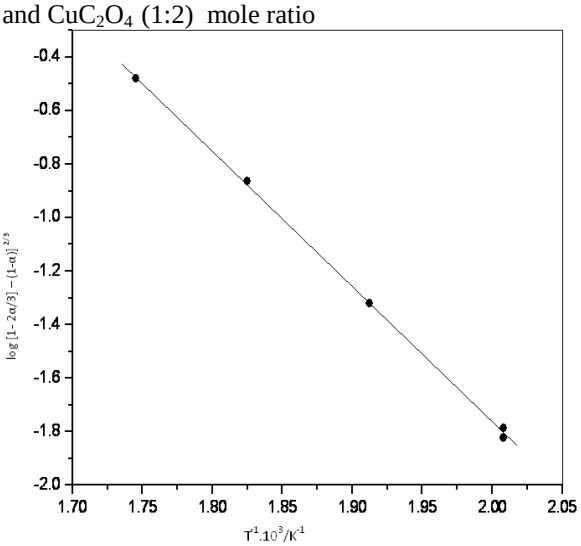

Fig14. Arrhenius plot for EGA of log [1- 2α/3] – (1-α)] **2/3** Vs $T^{-1}.10^3/K^{-1}$ for decomposition of $FeC_2O_4.2H_2O$ and CuC_2O_4 (1:2) mole ratio.

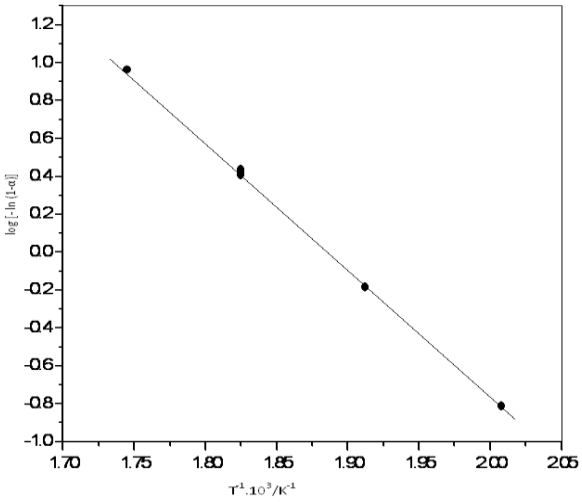

Fig15. Arrhenius plot for EGA of log [- ln (1-α)] Vs $T^{-1}.10^{3}/K^{-1}$ for decomposition of FeC2O4.2H2O and CuC2O4 (1:2) mole ratio.

The decomposition of binary mixture (Table1) using TGA can be found out by plotting [1- 2α/3] – (1-α)] $^{2/3}$ Vs. time (min) and [- ln (1-α)] Vs. time (min) (Figure 15 and Figure 16) and obey three dimensional diffusion (Braunshtein equation) (D_4) followed by first order kinetics (Mampel unimolecular law) or random nucleation. This means the fact that reaction is controlled by nucleation followed by growth, where the rate determining step is the nucleation process followed by diffusion control reaction starting on the exterior of a spherical particle. While using EGA, decomposition can be found same as TGA shown in (Figure 17 and Figure 18) [41].

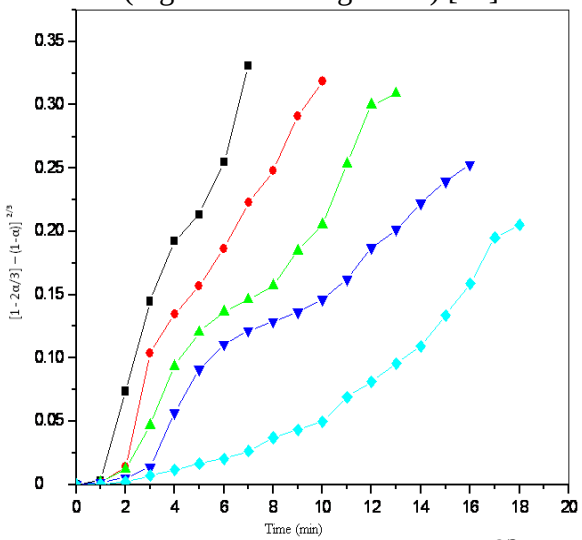

Fig16. (TGA) plot of [1- 2α / 3] – (1-α)] $^{2/3}$ Vs time of decomposition of $FeC_2O_4.2H_2O$ and CuC_2O_4 (1:2) mole ratio.

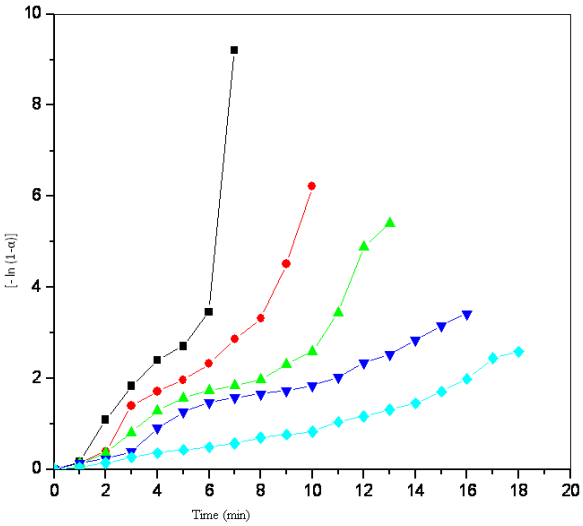

Fig17. (TGA) plot of [- ln (1-α)] Vs time of decomposition of $FeC_2O_4.2H_2O$ and CuC_2O_4 (1:2) mole ratio.

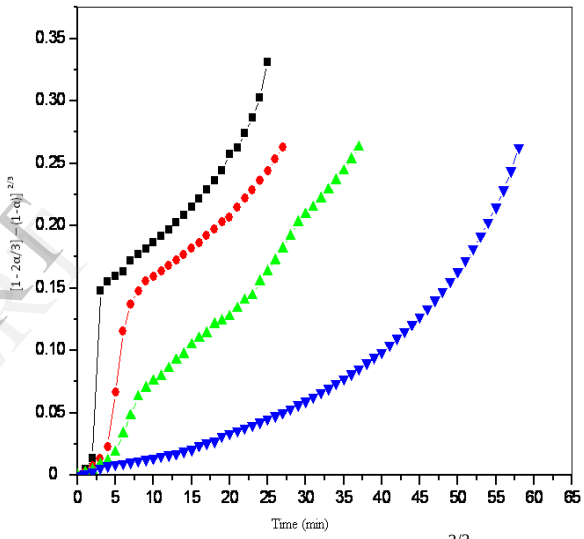

Fig18. (EGA) plot of [1- 2α / 3] –(1-α)] $^{2/3}$ Vs time of decomposition of $FeC_2O_4.2H_2O$ and CuC_2O_4 (1:2) mole ratio.

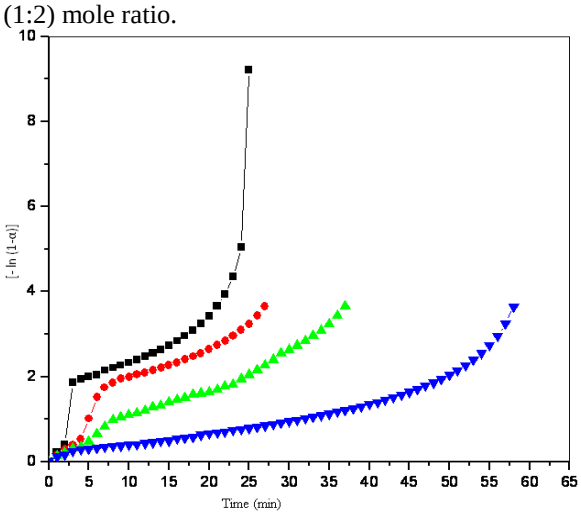

Fig19. (EGA) plot of [- ln (1-α)] Vs time of decomposition of $FeC_2O_4.2H_2O$ and CuC_2O_4 (1:2) mole ratio.

Table2: Activation parameters of the non-isothermal and isothermal decomposition in air of $FeC_2O_4.2H_2O$ and CuC_2O_4 by TGA and EGA method.

Method of analysis	Ea (activation energy) in KJ/mole.	A,(frequency factor)	r, (correlation coefficient)	n, Order of reaction
Non-isothermal TGA of Ferrous (II) oxalate.	176.33	$1.83x10^8$	0.9962	2.5
Isothermal TGA by two dimensional diffusion of Ferrous (II) oxalate.	136.07	$3.02x10^7$	0.9999	2.5
Isothermal TGA by three dimensional diffusion (Ginling Braunshtein equation) of Ferrous (II) oxalate.	138.09	$4.78x10^7$	0.9999	2.5
Non-isothermal EGA of Ferrous (II) oxalate.	98.80	$8.28x10^3$	0.9908	1.35
Isothermal EGA by two dimensional diffusion of Ferrous (II) oxalate.	93.89	$2.97x10^6$	0.9988	1.35
Isothermal EGA by three dimensional diffusion (Ginling Braunshtein equation) Ferrous (II) oxalate.	106.04	$5.85x10^6$	0.9995	1.35
Non-isothermal TGA of Copper (II) oxalate.	140.46	$1.95x10^6$	0.9948	1.35
Isothermal TGA by random nucleation (Avrami equation) of Copper (II) oxalate.	172.40	$1.95x10^6$	0.9999	1.35
Non-isothermal EGA of Copper (II) oxalate.	158.82	$1.56x10^3$	0.9994	0.35
Isothermal EGA by random nucleation (Erofeev equation) of Copper (II) oxalate.	144.31	$3.51x10^8$	0.9999	0.35

Conclusion

TGA experiment of $FeC_2O_4.2H_2O$ and CuC_2O_4 (1:2) mole ratio mixture in air shows complete decomposition to Fe_2O_3 and 2CuO at 260 °C through two well defined steps, while EGA technique shows the same decomposition at 300 °C. The initiation temperature of pure $FeC_2O_4.2H_2O$ and CuC_2O_4 are 240 °C and 260 °C and ends of temperature are 300 °C and 320 °C respectively. While binary mixture shows initiation temperature 220 °C and ends of temperature 260 °C this is due to the catalytic effect of CuO, which decreases decomposition temperature and activation energy (Ea).

Acknowledgements

The authors are grateful to the Head, Department of Chemistry and Principal, New Arts, Commerce and Science College, Ahmednagar for providing the all required facilities to carry out the work.

References

[1] Basma, A. A., and Balboul., 2000, "Thermal decomposition study of erbium oxalate hexahydrate, " Thermochimica. Acta., 351, pp. 55–60.

[2] Muraleedharan, K., Labeeb, P., Abdul Mujeeb, V. M., Aneeh, M. H., Ganga Devi, T., and Kannan, M. P., 2011, "Effect of particle size on non-isothermal decomposition of potassium titanium oxalate," Z. Phys. Chem., 225, pp. 169-181.

[3] Boldyrev, V. V., Bulens, M., Delmon, B., 1979, "The Control of the reactivity of Solids," Elseveir, Amsterdam.
[4] Majumdar, S., Sharma, I. G., Bidaye, A. C., Suri, A. K., 2008, "A study on isothermal kinetics of thermal decomposition of cobalt oxalate to cobalt," Thermochimica. Acta., 473, pp. 45-49.
[5] Shahheen, W. M., 2002, "Thermal solid-solid interaction and catalytic properties of CuO/Al_2O_3 system treated with ZnO and MoO_3," Thermochimica. Acta., 385, pp.105-116.
[6] Malecka, B., Drozdz-ciesla, E., Melecki, A., 2004, "Mechanism and kinetics of thermal decomposition of zinc oxalate," Thermochemica. Acta., 423, pp. 13-18.
[7] Palanisamy, T., Gpalakrishnan, J., Viswanathan, B., Srinivasanand, V., Sastri, M. V. C., 1971, "Kinetics of thermal decomposition of some metal oxalates,"Thermochimica.acta., 2(3), pp. 265-273.
[8] Nayak, H., Bhatta, D., 2001, "Thermal analysis of La-Ba oxalate and role of γ-irradiation there on," Thermochemica. Acta., 373, pp. 37-43.
[9] Górski, A., Kra´snicka, A. D., 1987, "The importance of the CO_2^{2-} anion in the mechanism of thermal decomposition of oxalates," J. Therm. Anal. Calorim., 32, pp. 1229–1241.
[10] Reddy, M. V. V. S., Lingam, K. V., Rao, T. K. G., 1981, "Radical studies in oxalate systems: E.S.R. of CO^{2-} in irradiated potassium oxalate monohydrate," Mol. Phys., 42, pp. 1267–1269.
[11] Leiga, A. G., 1966, "Decomposition of silver oxalate. II. Kinetics of the thermal decomposition," J. Phys. Chem., 70, pp. 3260–3267.
[12] Jose John1, M., Muralidharan, K., Kannan, M. P., Ganga Devi, T., 2012, "Effect of semiconducting metal oxide additives on the kinetics of thermal decomposition of sodium oxalate under isothermal conditions," Thermochim Acta., 534, pp. 71-76.
[13] El-Bellihi, A. A., 1994, "Kinetics of the non-isothermal decomposition of Cu-and Co-itaconato complexes," Journal of Thermal Analysis., 41, pp. 191-200.
[14] Gabal, M. A., 2004, "Non-isothermal studies for the decomposition course of CdC_2O_4-ZnC_2O_4 mixture in air," Thermochemica. Acta., 412, pp. 55-62.
[15] ARII, T., Motomura, K., and Otake, S., 2011, "Evolved gas analysis using photoionization mass spectrometry, EGA-PIMS: characterization of pyrolysis products from polymers," J. Mass Spectrom. Soc. Jpn., 59(1), pp. 5-11.
[16] Birzescu, M., Niculescu, M., Dumitru, R., Budru-geac, P., and Segal, E., 2008, "Copper (II) oxalate obtained through the reaction of 1, 2-ethanediol with Cu (NO_3) $2.3H_2O$," Journal of Thermal Analysis and Calorimetry., 94(1), pp. 297-303.
[17] Deane, K., Smith, and Jenkins, R., 1996, "JCPDS -International Centre for Diffraction Data, Newtown square, PA 19073, The powder diffraction file: past, present and future," Journal of Research of the National Institute of Standards and Technology., 101(3), pp. 259-271.
[18] Judd., M. D., and Pope, M. I., 1972, "High temperature superconductivity 1: Materials," Journal of Thermal. analysis., 4, pp. 31–38.
[19] Gao, X., and Dollimore, D., 1993, "The thermal decomposition of oxalates: Patr26. A kinetic study of the thermal decomposition of manganese (II) oxalate dehydrate," Thermochemica. Acta., 215, pp. 47-63.
[20] Wan-Jun, T., Dong-Hua, C., 2007, "Thermal decomposition kinetics of ferrous oxalate dehydrate," Acta. Phys. Chim. Sin., 23(04), pp. 605-608.
[21] Angermann, A., Topfer, J., 2008, "Synthesis of magnetite nanoparticles by thermal decomposition of ferrous oxalate dehydrate, " J. Mater. Sci., 43, pp. 5123-5130.
[22] Hermanec, M., Zboril, R., Machala, M., and Schneeweiss, O., 2006, "Thermal behavior of iron (II) oxalate dihydrate in the atmosphere of its conversion gases," Journal of Material Chemistry. 16, pp. 1273-1280.
[23] Lamprecht, E., Watkins, G. M., Brown, M. E., 2006, "The thermal decomposition of copper (II) oxalate revisited," Thermochemica. Acta., 446, pp. 91-100.
[24] Zhang, X., Zhang, D., Ni, X., Zheng, H., 2008. "Optical and electrochemical properties of nanosized CuO via thermal decomposition of copper oxalate," Solid State Electronics., 52, pp. 245-248.
[25] Dumitru, R., Carp, O., Budrugeac, P., Niculescu, M., segal, E., 2011, "Non-isothermal decomposition kinetics of $[CoC_2O_4.2.5H_2O]_n$," J. Therm. Anal. Calorim., 103(2), pp. 59-596.
[26] Dollimore, D., 1987, "The thermal decomposition of oxalates A Review," Thermochimica. Acta., 117, pp. 331-363.
[27] Gabal, M. A., 2003, "Kinetics of the thermal decomposition of CuC_2O_4 - ZnC_2O_4 mixture in air," Thermochimica . Acta., 402, pp. 199-208.
[28] Frost, Locke, R. L., Ashley, J., and Martens, Wayde, N., 2008, "Thermogravimetric analysis of wheatleyite Na_2Cu_2 + $(C_2O_4)_2.2H_2O$, " Journal of thermal Analysis and Calorimetry., 93(3), pp. 993-997.
[29] Yan, B., Zhang, H. J., Zhou, G. L., and Ni, J. Z., 2003, "Different thermal decomposition process of lanthanide complexes with N-phenyl anthranilic acid in air and nitrogen atmosphere," Chem. Pap., 57(2), pp. 83-86.
[30] Swanson., Tatge., and Natl., 1953, Bur. Stand. (US) Circ., 539(1), pp. 49.
[31] Antipin, M. Y., Nauk, D. A., 1985, SSSR, 281, pp. 854.

[32] Qusti, A. H., Samarkandy, A. A., A_L-$T_{HABAITI}$, S., and $D_{IEFALLAH}$ E_L-H, M., 1997, "The Kinetics of thermal decomposition of Nickel Formate Dihydrate in Air," JKAU. Sci., 9, pp. 73-81.
[33] Drouet, C., and Alphonse, P., 2002, "Synthesis of mixed manganites with high surface area by thermal decomposition of oxalates," J. Mater. Chem., 12, pp. 3058-3063.
[34] Boldyrev, V. V., 2002, "Thermal decomposition of silver oxalate," Thermochimica. Acta., 388, pp 63-90.
[35] Muraleedharan, K., and Pasha, L., 2011, "Thermal decomposition of potassium titanium oxalate," J. Serb. Chem. Soc., 76(7), pp. 1015-1026.
[36] Yu-Dong, Z., Bin-Jie, L., Xiang-Min, X., De-Liang, L., 2007, "Thermal decomposition Kinetics of $ZnSn(OH)_6$," Acta. Phsy. Chim. Sin., 23, pp. 1095-1098.
[37] L'vov, B.V., 2002, "The interrelation between the temperature of solid decomposition and the E parameter of Arrhenius equation," Thermochim. Acta., 389, pp. 199–211.
[38] Galwey, A. K., and Brown, M. E., 2002, "Applications of the Arrhenius equation to solid state kinetics: can this be justified?," Thermochim. Acta., 386, pp. 91-98.
[39] Coetzee, A., Brown, M. E., Eve, D. J., and Strydom, C. A., 1994, "Kinetics of the thermal dehydration and decomposition of some mixed metal oxalates," Journal of Thermal Analysis., 41, pp. 357 - 385.
[40] Nair, C. G. R., Mathew, S., and Ninan, K.N., 1989, "Thermal decomposition kinetics: part XVI. Kinetics and mechanism of thermal decomposition of diaquobis(ethylenediammine) copper (II) oxalate," Thermochemica. Acta., 150, pp. 63-78.
[41] Prasad, R., 2003, "Mechanism and kinetics of thermal decomposition of ammoniacal complex of copper oxalate," Thermochim. Acta., 406, pp. 99-104.